COMPUTATIONAL MECHANICS
New Trends and Applications
S. Idelsohn, E. Oñate and E. Dvorkin (Eds.)

AN EFFICIENT CONTINUOUS STRESS MIXED MODEL BASED ON THE REISSNER'S PRINCIPLE

Mladen Berković[*] and Dubravka Mijuca[†]

[*] Faculty of Mathematics
University of Belgrade
Akademski trg 16, P.O. Box 550, 11000 Belgrade, Yugoslavia
e-mail: berkovic@matf.bg.ac.yu

[†] Faculty of Mathematics
University of Belgrade
Akademski trg 16, P.O. Box 550, 11000 Belgrade, Yugoslavia
e-mail: dmijuca@matf.bg.ac.yu

Key words: primal mixed model, stress continuity.

Abstract. *In this paper a primal–mixed finite element approach based on the Reissner's principle is presented. A stable finite element mixed procedure is obtained by choosing the dual quantity from the space* $\left(H^1\right)^{n\times n}$ *and using different approximations for primal and dual quantities when the essential boundary conditions for the dual quantities are introduced. The present procedure results in a symmetric sparse system of linear equations, solvable by the symmetric Gaussian elimination, as in the case of classical finite element approach, thus giving a fair base for the comparison of the solution times. The main goal of this paper is to compare efficiency of the present primal–mixed finite element scheme with that of the classical finite element procedure, at least for the two–dimensional plane elasticity problems. After the extensive numerical examinations authors propose the mixed finite element procedure orders of magnitude more efficient than classical finite element displacement analysis. In the same time questionable post–processing routines for calculating dual quantities of interest are avoided.*

1 INTRODUCTION

Contemporary finite elements are often based on some of formulations that can be called ‘mixed’, in a sense that, at variance with the classical (primal) finite element method where fundamental unknowns (in the mechanics of solids) are displacements only, the fundamental variables can be also stresses and/or strains.

At a glance, mixed methods have some serious drawbacks. For instance, a fact that discrete mixed method system involves more degrees of freedom than primal one, and hence the unacceptable execution time for the *same mesh*, is considered as one of main disadvantages of mixed methods. However, in this paper it will be shown that the present mixed model is (orders of magnitude) faster than classical finite element analysis for the *same accuracy*. Further, the classical approach, based on an extremal principle, has a positive definite system matrix. On the contrary, as a saddle point problem, mixed approach leads to an indefinite system of algebraic equations, thus narrowing the number of solution techniques that can be applied directly. However, a usual sparse Gaussian elimination solver can be, and has been, successfully used for the solution of the resulting systems of equations of the proposed procedure.

The present, primal–mixed procedure is based on rather uncommon mixed formulation, similar in principle to that in Zienkiewicz and Taylor[1], but having both the displacement *and* stress boundary conditions exactly satisfied.. The main goal of this paper is to show that the proposed procedure is easy for implementation and more efficient in the sense of the execution time needed for the prescribed accuracy than classical finite element procedure.

2 MATHEMATICAL MODEL

We use the weak formulation of a mixed problem, associated with Reissner's variational principle[1,2]:

Find $\boldsymbol{T} \in \left(L_2\right)^{n\times n}$ and $\boldsymbol{u} \in \left(H^1\right)^n$ such that $\boldsymbol{u}\big|_{\partial B_t} = \boldsymbol{w}$ and

$$\int_{\mathrm{B}} (\boldsymbol{A}\boldsymbol{S}:\boldsymbol{T} - \boldsymbol{S}:\nabla\boldsymbol{u} - \nabla\boldsymbol{v}:\boldsymbol{T})dV = -\int_{\mathrm{B}} \boldsymbol{v}\cdot\boldsymbol{f}\,dV - \int_{\partial \mathrm{B}_t} \boldsymbol{v}\cdot\boldsymbol{p}\,dA \tag{1}$$

for all $\boldsymbol{S} \in \left(L_2\right)^{n\times n}$ and $\boldsymbol{v} \in \left(H^1\right)^n$ such that $\boldsymbol{v}\big|_{\partial \mathrm{B}_t} = 0$.

In this expression $\boldsymbol{T}$ is the stress tensor, $\boldsymbol{f}$ the vector of the body forces, $\boldsymbol{u}$ the displacement vector, $\boldsymbol{A}$ the elastic compliance tensor, $\boldsymbol{p}$ the vector of the boundary tractions, and $\boldsymbol{w}$ the vector of the prescribed displacements. Because the displacement spaces are the same as in the classical displacement approach, and the stress space can be discontinuous at the element boundaries, it is a straightforward task to construct the elements of the above type. However, it is possible to consider also the continuous stress space, i.e. $\boldsymbol{T} \in \left(H^1\right)^{n\times n}$, the space of all symmetric tensorfields that have square integrable gradient. This approach has been succesfully used by Mirza and Olson[3,4] for linear triangles, and by the present first author and Drašković[5] for bilinear isoparametric quadrilaterals. Numerical results indicated high accuracy of a model. Moreover, the direct treatment of stress constraints as essential boundary conditions[6,7], albeit not always necessary, is also possible and useful in the framework of the formulation (1).

3 FINITE ELEMENT SUBSPACES

We let $\mathcal{C}_h$ be the partitioning of $\mathcal{B}$ into elements $\mathcal{E}$ and define the finite element subspaces for the displacement vector, the stress tensor and the appropriate weight functions respectively as:

$$\boldsymbol{U}_h = \{\boldsymbol{u} \in \left(H^1\right)^n(\mathcal{B}) \;\Big|\; \boldsymbol{u}\big|_{\partial \boldsymbol{B}_u} = \boldsymbol{w}, \quad \boldsymbol{u}\big|_{\boldsymbol{E}} = U^K(\mathcal{E})\boldsymbol{u}_K, \quad \forall \mathcal{E} \in \mathcal{C}_h\}, \tag{2}$$

$$\boldsymbol{T}_h = \{\boldsymbol{T} \in \left(H^1\right)^{n\times n}(\mathcal{B}) \;\Big|\; \boldsymbol{Tn}\big|_{\partial \boldsymbol{B}_t} = \boldsymbol{p}, \quad \boldsymbol{T}\big|_{\boldsymbol{E}} = T_L(\mathcal{E})\boldsymbol{T}^L, \quad \forall \mathcal{E} \in \mathcal{C}_h\}, \tag{3}$$

$$\boldsymbol{V}_h = \{\boldsymbol{v} \in \left(H^1\right)^n(\mathcal{B}) \;\Big|\; \boldsymbol{v}\big|_{\partial \boldsymbol{B}_u} = 0, \quad \boldsymbol{v}\big|_{\boldsymbol{E}} = V^M(\mathcal{E})\boldsymbol{u}_M, \quad \forall \mathcal{E} \in \mathcal{C}_h\}, \tag{4}$$

$$\boldsymbol{S}_h = \{\boldsymbol{S} \in \left(H^1\right)^{n\times n}(\mathcal{B}) \;\Big|\; \boldsymbol{Sn}\big|_{\partial \boldsymbol{B}_t} = 0, \quad \boldsymbol{S}\big|_{\boldsymbol{E}} = S_L(\mathcal{E})\boldsymbol{T}^L, \quad \forall \mathcal{E} \in \mathcal{C}_h\}. \tag{5}$$

In these expressions $\boldsymbol{u}_K$ and $\boldsymbol{T}^L$ are the nodal values of the vector $\boldsymbol{u}$ and tensor $\boldsymbol{T}$ respectively. Accordingly, U^K and T_L are the corresponding values of the interpolation functions, connecting the displacements and stresses at an arbitrary point in $\mathcal{E}$ (the body of an element), and the nodal values of these quantities. The complete analogy holds for the displacement and stress variations (weight functions) $\boldsymbol{v}$ and $\boldsymbol{S}$ respectively.

4 COMPACT MATRIX FORM OF THE FINITE ELEMENT EQUATIONS

As it has been shown by Berković and Drašković[6], a suitable choice of the local boundary coordinate systems enables us to find one–to–one correspondence between the prescribed boundary tractions and some of the stress components, i.e., $\mathbf{t}_p$ (prescribed) at a boundary and a problem under consideration based on (1) can be formulated as:

$$\begin{bmatrix} \mathbf{A}_{vv} & -\mathbf{D}_{vv} \\ -\mathbf{D}_{vv}^T & 0 \end{bmatrix}\begin{bmatrix} \mathbf{t}_v \\ \mathbf{u}_v \end{bmatrix} = \begin{bmatrix} -\mathbf{A}_{vp} & \mathbf{D}_{vp} \\ \mathbf{D}_{pv}^T & \mathbf{0} \end{bmatrix}\begin{bmatrix} \mathbf{t}_p \\ \mathbf{u}_p \end{bmatrix} - \begin{bmatrix} \mathbf{0} \\ \mathbf{F}_p + \mathbf{P}_p \end{bmatrix}. \tag{6}$$

In this expression unknown (variable) stresses $\mathbf{t}_v$ and displacements $\mathbf{u}_v$, and the known (prescribed) ones $\mathbf{t}_p$ and $\mathbf{u}_p$, are separated. Furthermore, the nodal stress $\mathbf{t}^{Lst}$ and displacement u_{Kq} components are consecutively ordered in the column matrices $\mathbf{t}$ and $\mathbf{u}$ respectively. The members of the matrices **A** and **D** and of the vectors (column matrices) **F** and **P** (discretized body and surface forces) are respectively:

$$A_{NuvLst} = \sum_{\mathcal{e}} \int_{\mathcal{E}} S_N g^a_{(N)u} g^b_{(N)v} A_{abcd} g^c_{(L)s} g^d_{(L)t} T_L \mathrm{d}V, \tag{7}$$

$$D_{Nuv}^{Kq} = \sum_{e} \int_{E} S_N U_a^K g_{(N)u}^{a} \mathrm{d}V g_{(N)v}^{(K)q}, \tag{8}$$

$$F^{Mq} = \sum_{e} \int_{E} g_a^{(M)q} V^M f^a \mathrm{d}V, \tag{9}$$

$$P^{Mq} = \sum_{e} \int_{\partial E_t} g_a^{(M)q} V^M p^a \mathrm{d}A, \tag{10}$$

where

$$g_{(L)s}^{(K)m} = \delta_{kl} g^{(K)mn} \frac{\partial z^k}{\partial x^{(K)n}} \frac{\partial z^l}{\partial y^{(L)s}}, \tag{11}$$

$$g_{(L)s}^{a} = \delta_{kl} g^{ab} \frac{\partial z^k}{\partial \xi^b} \frac{\partial z^l}{\partial y^{(L)s}}, \tag{12}$$

$$g_{b}^{(K)q} = \delta_{kl} g^{(K)qp} \frac{\partial z^k}{\partial \xi^b} \frac{\partial z^l}{\partial x^{(K)p}}, \tag{13}$$

are the Euclidean shifters. In these expressions z^i (i, j,k,l = 1,2,3) are the global Cartesian coordinates, while $x^{(K)n}$ (m,n,p,q = 1,2,3) and $y^{(L)s}$ (r,s,t,u,v = 1,2,3) are local (nodal) coordinates, used for the determination of the nodal displacements and stresses respectively. Commonly used notions, $\xi^a (a,b,c,d = 1,2,3)$ are taken for the local (element) coordinates, usually convected (parametric, isoparametric). Further, $g^{(K)mn}$ and g^{ab} are the components of the contravariant fundamental metric tensors, the first one with respect to $x^{(K)n}$ and the second to ξ^b. Computation of these quantities is described in detail per instance in [2]. Furthermore, $U_a^K = \partial U^K / \partial \xi^a$. Finally, A_{abcd} are the components of the elastic compliance tensor A, while f^a and p^a are the body forces and boundary tractions, respectively. Integration is performed over the body $\mathcal{E}$ of each element, or over the part of the boundary surface $\partial \mathcal{E}_t$ where the tractions are given, while summation is over all the elements $\boldsymbol{e}$ of a system.

Because the tensorial character of (1) is fully respected, in a sense introduced by Drašković[8], one can choose at each global node different coordinate systems for the stresses and/or displacements, for the most convenient application of the boundary conditions and interpretation of the output results.

5 SOLVABILITY OF A SYSTEM

When solvability and stability of a solution of (6) are considered, LBB (Ladyzhenskaya, Babuska, Brezzi) condition[9] is often cited. Here some of its algebraic implications will be elaborated. In the accordance with Carey and Oden[10] p. 134, if LBB is to hold, we should have

$$\dim \boldsymbol{T}_h \geq \dim \nabla \boldsymbol{U}_h. \tag{14}$$

In the present context

$$\nabla \boldsymbol{U}_h = \{2\boldsymbol{e}_h = \nabla \boldsymbol{u}_h + \nabla \boldsymbol{u}_h^t, \ \boldsymbol{u}_h \in \boldsymbol{U}_h\}, \tag{15}$$

is evidently a *strain* subspace. Let us discuss now the dimensions (number of entries) of the finite element spaces under consideration. In the absence of the boundary conditions, and if the same mesh is used for both the displacements and stresses, taking also into account the symmetry of the stress tensor, the dimensions of the displacement, strain and stress spaces will be respectively:

$$n_u = \dim \boldsymbol{U}_h = n\,N_u; \quad n_t = \dim \boldsymbol{T}_h = \tfrac{1}{2} n(n+1)\,N_t;$$
$$n_e = \dim \nabla \boldsymbol{U}_h = \tfrac{1}{2} n(n+1)\,N_u. \tag{16}$$

Certainly, $\boldsymbol{T}_h$ and $\nabla \boldsymbol{U}_h$ are the spaces of the second order tensors. Each of these tensors has $n(n+1)/2$ components, where n is the number of spatial dimensions of the problem under consideration. Furthermore, N_t is the number of nodes of a *stress mesh*, while N_u is the number of nodes of a *displacement mesh*. From (14) and (16) it follows directly that, in the absence of the stress boundary conditions, (14) will be satisfied if

$$N_t \geq N_u. \tag{17}$$

This relationship justifies the relative success of the scheme[1,3,4,5], where $N_t \equiv N_u$. Let us note also that, because at each node of a stress mesh we have (due to the symmetry of a stress tensor) $n(n+1)/2$ stress degrees of freedom, and at each node of a displacement mesh n displacement degrees of freedom, the well–known condition[1]

$$n_t \geq n_u, \tag{18}$$

can be rewritten as

$$\frac{1}{2} n(n+1)\,N_t \geq n\,N_u. \tag{19}$$

If (17) holds, (19) will be satisfied for any and every value of n. However, the reverse is not true. Consequently, (17) is a stronger condition than (18) and hence more helpful in giving ideas how to construct and modify the trial space to maintain solvability. Note however that in *one-dimensional* ($n = 1$) case the aforementioned conditions are equivalent.

If (some or all) of the stress boundary conditions are enforced, the number of unknown nodal stresses in (6) is decreased. Hence, the conditions (14) and consequently (17) are endangered. In practice, this means that the solution of (6) is likely to fail. To eliminate the problem one can apply, instead of (17), a somewhat conservative heuristic rule

$$N_t - N_t^* \geq N_u. \tag{20}$$

In this expression, N_t^* is the number of nodes having at least one of the stress components prescribed. It is evident that (20) cannot be satisfied for $N_t = N_u$ i.e. if the same mesh is used for both the displacements and stresses. Hence it is necessary to enrich the stress mesh by the additional nodes. Note that, due to Arnold[2], enrichment of the space $\boldsymbol{T}_h$ increases stability of a solution. More details will be given in the discussion on the numerical example.

6 SOME DETAILS OF THE SOLUTION PROCEDURE

For the sake of the better insight into the solution procedure, the two-dimensional model problem will be considered. In that case for the each mutually interconnected (by the common element(s)) pair of nodes L and M, or L and K, respectively, submatrices of **A** and **D** have the following structure:

$$A_{LstMuv} = \begin{bmatrix} A_{L11M11} & 2A_{L11M12} & A_{L11M22} \\ A_{L12M11} + A_{L21M11} & 2A_{L12M21} + 2A_{L21M12} & A_{L12M22} + A_{L21M22} \\ A_{L22M11} & 2A_{L22M12} & A_{L22M22} \end{bmatrix}, \tag{21}$$

$$D_{Lst}^{Kq} = \begin{bmatrix} D_{L11}^{K1} & D_{L11}^{K2} \\ D_{L12}^{K1} + D_{L21}^{K1} & D_{L12}^{K2} + D_{L21}^{K2} \\ D_{L22}^{K1} & D_{L22}^{K2} \end{bmatrix}. \tag{22}$$

In these expressions indices 1 and 2 correspond to the displacements at the node K, while the indices 11, 12, 21 and 22 correspond to the stresses at nodes L and/or M.

The first main programming step in the above problem is an assembly procedure of the left and right sides of (6). The second one is the solution procedure of the resulting system (6).

The most natural and fastest way in the assembly procedure of (21) and (22) is to loop through the elements with putting in connection pairs of nodes L and M. At the left side of (6) the unconstrained degrees of freedom (components $\mathbf{t}_v$ and $\mathbf{u}_v$) connected with the current node L are retained. In contrary, at the right side the terms connected with the known components $\mathbf{t}_p$ and $\mathbf{u}_p$) are situated. The rows and columns connected with the components with zero $\mathbf{t}_p$ and $\mathbf{u}_p$ are neglected. The assembly procedure has been performed using the loops over the tensorial indices in (7) and (8). This technique looks to be more efficient than matrix reformulation of those expressions.

The matrix on the left side of (6) is indefinite, but it is also symmetric and sparse. Consequently, the symmetric sparse Gaussian elimination procedure can be used for the solution. Zeroes at the main diagonal of the left side are not an obstacle because triangularization procedure fills these positions with nonzero values.

It has been shown by the numerical examples that, despite the fact that the resulting system (6) is obviously larger than in the classical finite element analysis the efficiency of the procedure, measured as the accuracy versus the solution time, is in favor of the mixed formulation.

7 NUMERICAL EXAMPLE

Numerical experiments were conducted on the plane stress linear isotropic elasticity model problems. In order to form the stable system of algebraic equations, the considerations from the Section **5** were taken into account. If there is no traction boundary conditions, the bilinear shape functions for both displacements and stresses are sufficient to maintain the stability of a solution. On the other hand, when essential traction boundary conditions are introduced, number N_t has to be increased (usually by a central, ‘bubble’ node or by all additional five hierarchic quadratic nodes, in some or in all elements) to satisfy (20).

An efficient and stable solution procedure is obtained by reordering of nodes in that way that degrees of freedom connected with additional nodes always appear first in the solution procedure. Note that this is nothing else than a nested dissection ordering.

The present procedure, based on a primal–mixed scheme, was compared with the displacement type procedure based on a primal scheme. In the case of the displacement procedure, stresses were calculated *a posteriori* (in the postprocessing part of the finite element analysis) either with local stress smoothing by averaging the stresses at global nodes or by the global projection procedure[11].

The problem under consideration[12], Fig. 1, is a square plate of the unit semispan, with a central circular hole of the unit diameter. The plate is loaded along its sides by the unit load, tensile in horizontal, and compressive in vertical directions. Modulus of elasticity and Poisson's coefficient are taken to be $E = 1$ and $\nu = 0.3$ respectively. Because this model problem is geometrically symmetric and present method is coordinate independent (essential displacement and stress boundary conditions can be applied on any (e.g. skew or curved shape of the boundary) one–quarter (Fig. 1) and also one–eighth of it has been considered. Various mesh densities were examined. The appropriate coordinate systems are shown on the Fig. 2.

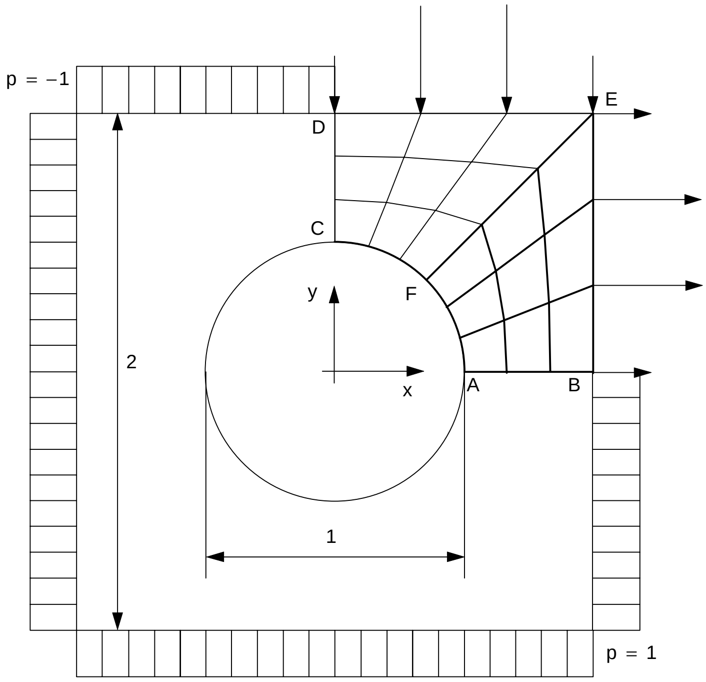

Figure 1: Square plate wih a circular hole

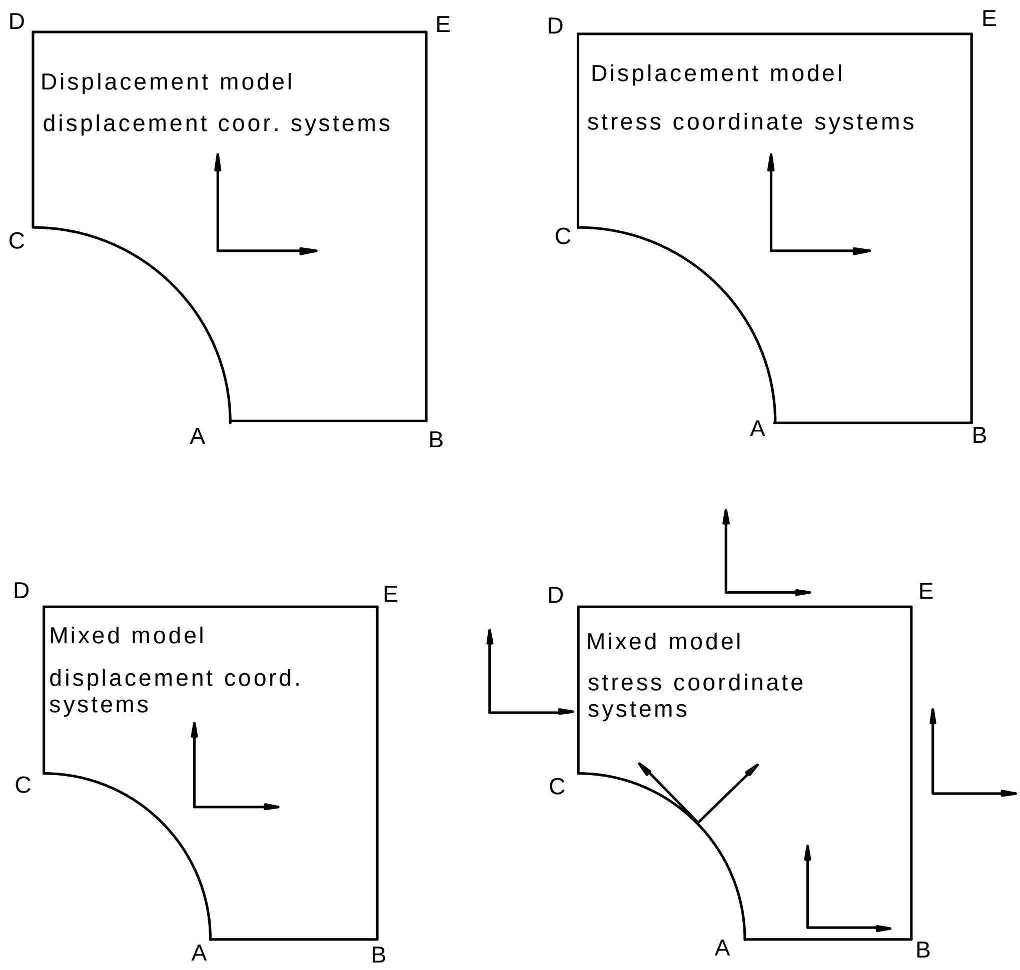

Figure 2: Square plate wih a circular hole. Coordinate systems

To get an idea about the stress and displacement behavior, the stress value $\mathrm{t} = t^{xx}$ at the point C is followed, which is positive and hence equals to the supreme norm (because of the extremal value of the stress at that point), and the largest displacement value $\mathrm{u} = u_x$ at a point B. Converged values of these stress and displacement are approximately $\mathrm{t} = 10.364$ and $\mathrm{u} = 6.4358$. The first value is slightly at variance with the reference[12] one $\mathrm{t} = 10.385$. For the strain energy the extrapolated value of 3.58275 is taken. The least squares extrapolation, based on the numerical results (using six significant digits) for several meshes, has been used for the determination of the 'converged values'.

In the Fig. 3. the stress convergence of the classical and present finite element approach is given. It can bee seen that in the classical (primal, 'displacement') approach stress crosses the converged value, and afterwards approaches it from above. At variance with this situation, mixed model converges uniformly (and more accurately) from below.

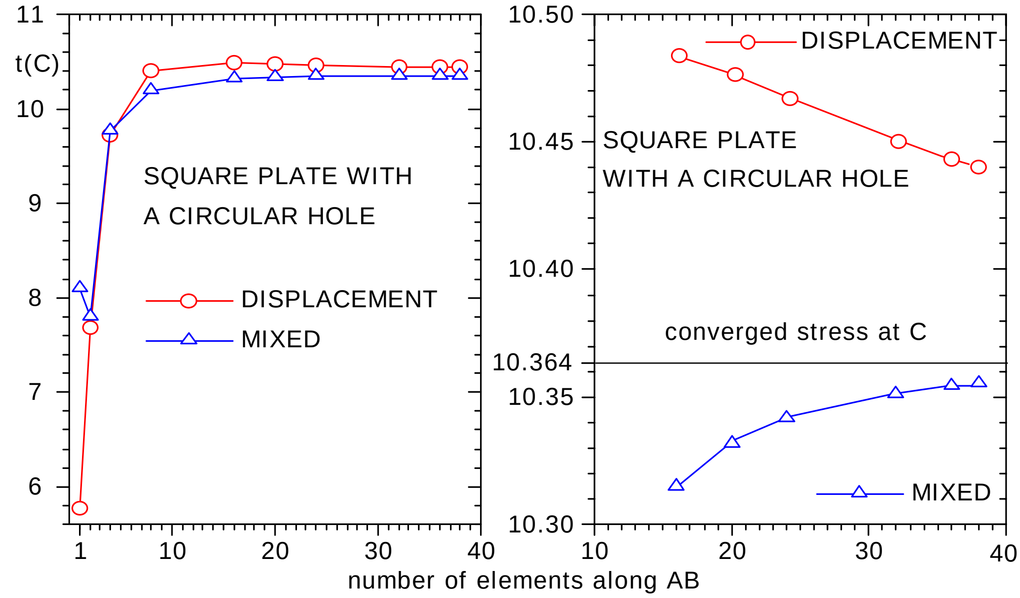

Figure 3: Stress convergence

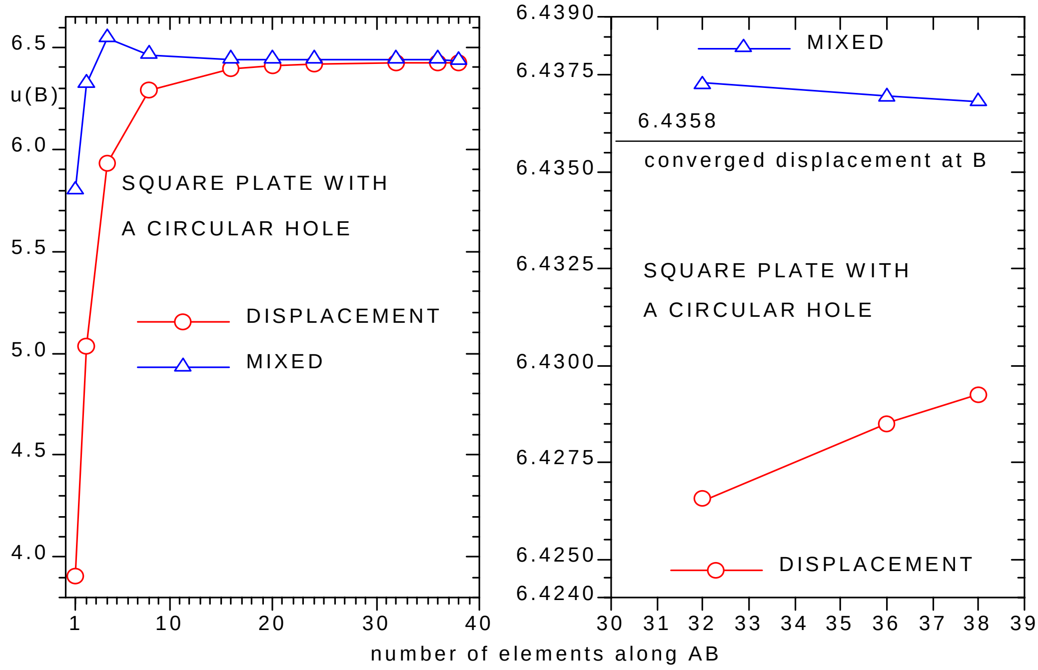

Figure 4: Displacement convergence

Similarly, in Fig. 4 the displacement convergences of the classical and present finite element approach are given. Here the mixed approach is again much more accurate. However, the maximum displacement for the mixed model converges from above, while for the displacement model it converges from below. One can conclude that the mixed model is evidently more accurate, and *less stiff* than the displacement model.

Obviously, this behavior of a solution can be considered as local, in the stress concentration area. For the better insight into the nature of a solution, an additional test has been performed, concerning the convergence in energy (Fig. 5). Not surprisingly, the convergence in energy is almost exactly quadratic for all models, as it should be expected on the basis of *a priori* error estimates for bilinear finite element subspaces. However, the accuracy is definitively in favor of the mixed model with the stress boundary conditions exactly satisfied. For the same displacement mesh, the relative error is almost an order of magnitude smaller than for standard finite element analysis.

But, some preliminary calculations show that the number of arithmetic operations can be an order of magnitude larger than for the classical finite element analysis over the same mesh. Hence, from the point of view of of the computational efficiency, an additional more detailed study, taking into account the solution time, should be performed for the fair comparison of these approaches. The results of this study, performed on a PC 486, are shown on the Fig. 6.

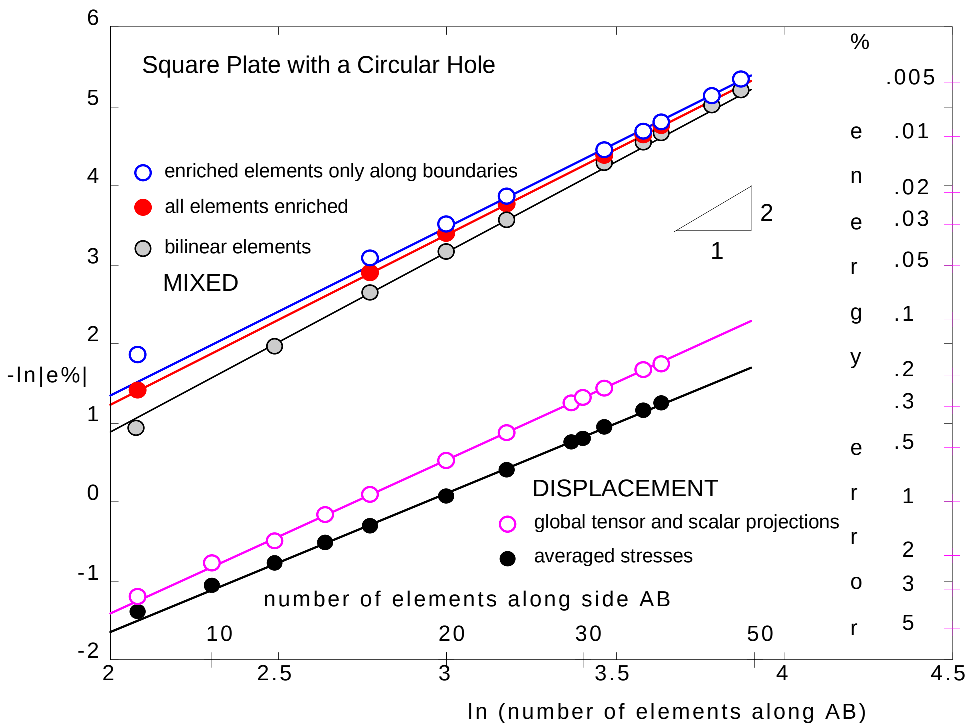

Figure 5: Relative error of strain energy versus number of elements along side AB

From the Fig. 5 and Fig 6 it can be concluded that the case with the stress bubble nodes located only in elements along a physical boundary is superior over the case when we have bubble nodes in all elements, and also over the simple bilinear approach without boundary tractions conditions applied. Anyhow, all these approaches are clearly superior compared with the classical analysis, irrespectively on the method of postprocessing used in that procedure.

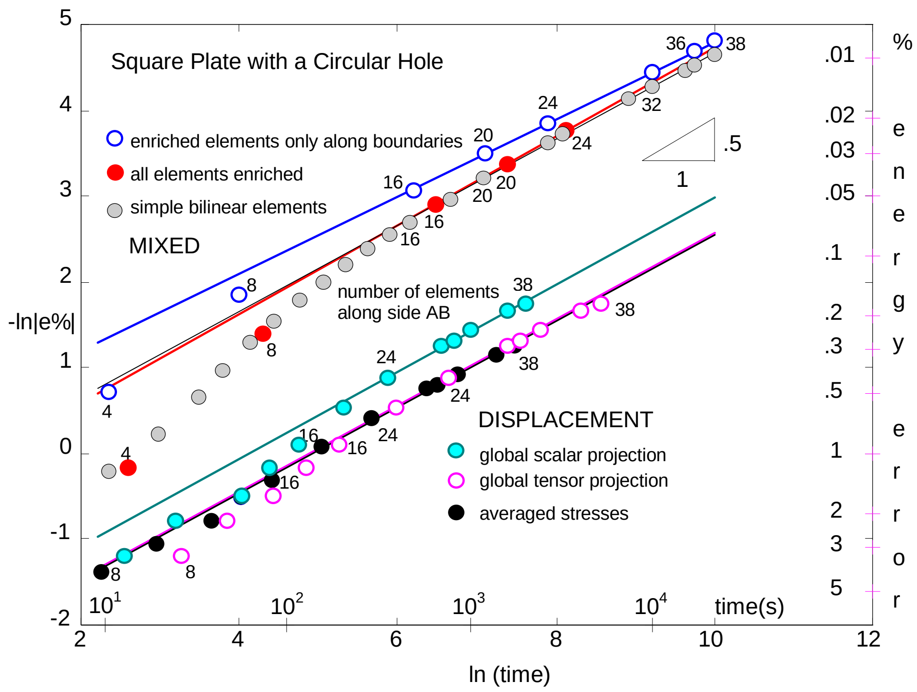

Fig. 6: Relative error of strain energy versus execution time

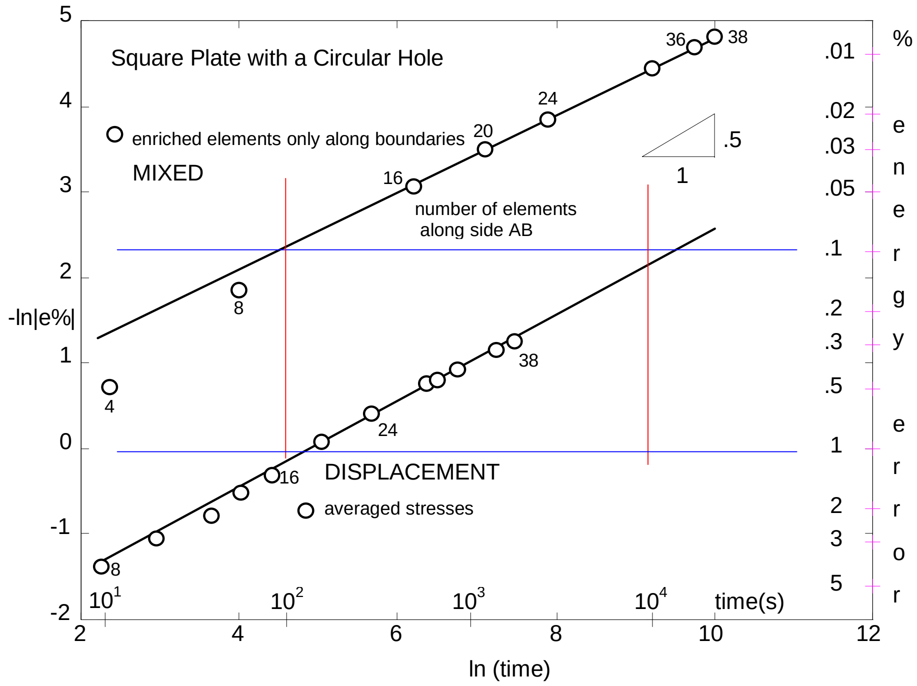

Figure 7: Comparison of the efficiencies of the classical and primal–mixed approaches

This superiority has been quantified on the simplified Fig. 7. It is evident that, for the same execution time, the accuracy of the mixed approach is approximately an order of magnitude higher than that of the classical analysis. Moreover, for the same accuracy required, execution is two orders of magnitude faster if the mixed analysis is used.

9 CONCLUSIONS

A primal-mixed finite element scheme is considered. The main goal was to investigate the possibility of achieving higher efficiency of the finite element analysis, and to prove it by the numerical examinations. On the basis of the above analysis and the numerical results, one can conclude, first, that the mixed elements with complete continuity can be practically realized, second, that simple and clear measures for the enhancement of the stability of a solution of the resulting equations are available, and finally, that the present mixed procedure is about *two orders of magnitude* more efficient than the classical finite element analysis

REFERENCES

[1] O.C. Zienkiewicz and R.L. Taylor, *The finite element method*, McGraw Hill, Vol. I., (1989).

[2] D.N.Arnold, "Mixed finite element methods for elliptic problems", *Comput. Methods Appl.. Mech. Engrg.*, **82,** 281-300 (1990).

[3] F.A. Mirza and M.D. Olson, "The mixed finite element in plane elasticity", *Int. J. Num. Meth. Engng.*, **15**, 273-289 (1980).

[4] M.D. Olson, "The mixed finite element method in elasticity and elastic contact problems", in S.N. Atluri, R.H.Gallagher and O.C.Zienkiewicz, eds., *Hybrid and Mixed Finite Element Methods*, John Wiley & Sons, 19-49 (1983).

[5] M. Berković and Z. Drašković, "Stress continuity in the finite element analysis", in J. Robinson, ed., *Accuracy, Reliability and Training in FEM Technology*, Robinson and Associates, 110-118 (1984).

[6] M. Berković and Z. Drašković, "On the essential mechanical boundary conditions in two-field finite element approximations", *Comput. Methods Appl. Mech. Engrg.*, **91,** 1339-1355 (1991).

[7] M. Berković and Z.V. Drašković, "A two-field finite element model related to the Reissner's principle", *Teorijska i Primenjena Mehanika*, **20,** 17-36 (1994).

[8] Z. Drašković, "On invariance of finite element approximations", *Mechanika Teoretyczna i Stosowana*, **26**, 597–601 (1988).

[9] F. Brezzi and M. Fortin, *Mixed and Hybrid Finite Element Methods,* Springer–Verlag, (1991).

[10] G. Carey and J.T. Oden, *Finite Elements: A Second Course*, Prentice–Hall, (1983).

[11] D. Mijuca, Z. Drašković and M. Berković, "Displacement Based Stress Recovery Procedure", *Advances in Finite Element Technology*, Civil-Comp Press, 127–134 (1996).

[12] A. K. Rao, I. S. Raju and A. V. Krishna Murty, "A powerful hybrid method in finite element analysis", *Int. J. Num. Meth. Engng,* **3**, 389–403 (1971).